Semiconductor Science and Technology

LETTER TO THE EDITOR

# Aharonov–Bohm oscillations of a tuneable quantum ring

INSTITUTE OF PHYSICS PUBLISHING SEMICONDUCTOR SCIENCE AND TECHNOLOGY
Semicond. Sci. Technol. **17** (2002) L22–L24 PII: S0268-1242(02)32811-6

## LETTER TO THE EDITOR

# Aharonov–Bohm oscillations of a tuneable quantum ring

**U F Keyser[1], S Borck[1], R J Haug[1], M Bichler[2], G Abstreiter[2] and W Wegscheider[3]**

[1] Institut für Festkörperphysik, Universität Hannover, Appelstr. 2, 30167 Hannover, Germany
[2] Walter Schottky Institut, TU München, 85748 Garching, Germany
[3] Angewandte und Experimentelle Physik, Universität Regensburg, 93040 Regensburg, Germany

E-mail: keyser@nano.uni-hannover.de

Received 17 January 2002
Published 12 April 2002
Online at stacks.iop.org/SST/17/L22

**Abstract**
Using an atomic force microscope a ring geometry with self-aligned in-plane gates was directly written into a GaAs/AlGaAs heterostructure. Transport measurements in the open regime show only one transmitting mode and Aharonov–Bohm oscillations with more than 50% modulation are observed in the conductance. The tuning via in-plane gates allows one to study the Aharonov–Bohm effect in the whole range from the open ring to the Coulomb-blockade regime.

The Aharonov–Bohm (AB) effect [1] has attracted much research interest over recent years in mesoscopic semiconductor physics. Several groups realized lateral AB rings [2–4] in heterostructures using well established techniques such as electron beam lithography and various etching techniques. Recently Piazza *et al* [5] realized a vertical AB interferometer which showed oscillations with amplitudes of 30%. Several groups used AB rings as phase detectors for the transport through quantum dots situated in one arm of the ring [6, 7]. Measurements on the spectrum of quantum rings were also performed with optical methods [8, 9].

Here we present data measured on an asymmetric quantum ring with two tuneable point contacts. The ring was fabricated using an atomic force microscope (AFM) as a nanolithographic tool. The design of the quantum ring enables us to measure electron interference effects and single-electron charging effects on the same device. In the open regime (resistance of contacts $R \approx h/e^2$) the quantum ring acts as an electron interferometer and we observe AB oscillations with a modulation amplitude of more than 50%. When the point contacts are pinched off ($R \gg h/e^2$) the ring is separated from the leads by tunnelling barriers. Because of the small diameter we can measure the typical Coulomb-blockade (CB) oscillations expected for a single-electron transistor. In addition, also we observe AB-like oscillations in this regime.

The fabrication was performed on a GaAs/AlGaAs heterostructure consisting of a 5 nm thick GaAs cap layer, 8 nm of AlGaAs, the Si-$\delta$-layer, a 20 nm wide AlGaAs barrier and 100 nm of GaAs (from top to bottom). The two-dimensional electron gas (2DEG) is located 34 nm below the surface with a density of $4.3 \times 10^{15}$ m$^{-2}$ and a mobility of 42 m$^2$ V$^{-1}$ s$^{-1}$. The mean free path of the electrons is 4.6 $\mu$m. A Hall-bar geometry was defined by standard photolithography and wet-chemical etching. The electron gas was then contacted with alloyed Au/Ge-contacts.

For the nanolithography of our samples we use local anodic oxidation with an AFM. It was shown by Ishii and Matsumoto [10] that shallow 2DEGs are depleted when the surface is oxidized using a conducting AFM tip. Held *et al* [11] demonstrated the very short depletion length (less than 50 nm) of this process. To obtain insulating lines with a breakdown voltage of $\pm$300 mV we apply high oxidation currents ($I \approx 1.0$ $\mu$A) and write the structures at least twice. Thus we create a lateral structure with self-aligned in-plane gates (IPGs). For more details on our current-controlled local oxidation see [12].

In figure 1(*a*) an AFM image of the geometry is shown. The oxide lines appear as a rough white–black surface (linewidth < 120 nm). With the oxide lines we define self-aligned IPGs. These are labelled as IPGA, IPGB and the

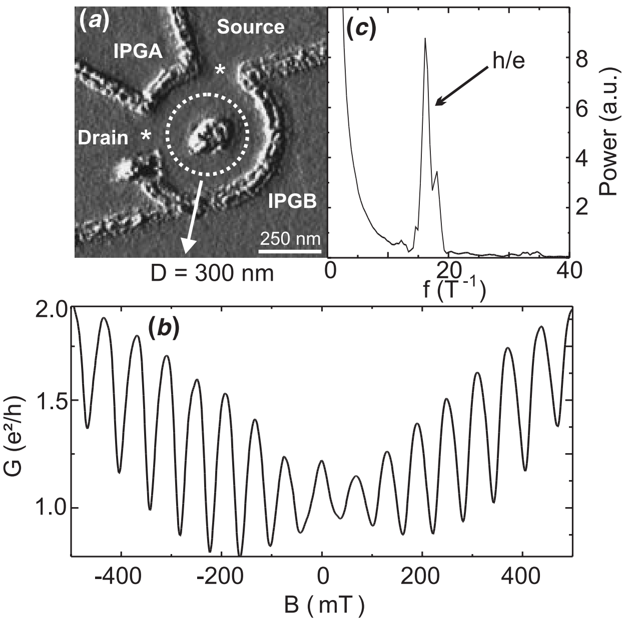


**Figure 1.** (*a*) AFM image of the ring structure. IPGA, IPGB denote the IPGs. The two point contacts are marked with an ∗. The white dashed circle (diameter 300 nm) corresponds to the transmitted mode extracted from (*b*) and (*c*). The inner diameter of the ring is $D_i = 190$ nm and the outer $D_o = 450$ nm. (*b*) Measurements of the conductance $G$ through the ring in perpendicular magnetic field $B$ ($V_A = 95$ mV, $V_B = 120$ mV, $T = 25$ mK). (*c*) Power spectrum of the measurement in (*b*).

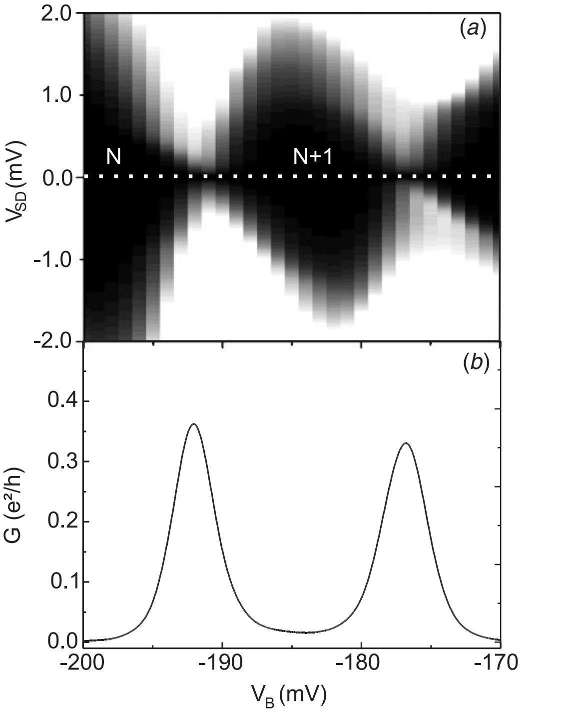


**Figure 2.** (*a*) Greyscale plot of the source–drain current $I_{SD}$ as function of $V_B$ and source–drain voltage $V_{SD}$ (grid size: $\Delta V_{SD} = 10\ \mu$V and $\Delta V_B = 1.0$ mV). White corresponds to $I_{SD} > 5$ nA and black to $I_{SD} < 0.1$ nA. The CB diamond indicates a charging energy of approximately 1 meV. (*b*) Conductance $G$ at $V_{SD} = 0$ mV through the quantum ring. Two CB peaks are shown.

applied voltages as $V_A$, $V_B$. We chose the inner diameter of the quantum ring as $D_i = 190$ nm and the outer diameter $D_o = 450$ nm. Thus the outer circumference of our ring is more than three times shorter than the mean free path in the unpatterned 2DEG. We can assume that we are in the ballistic regime and neglect effects of elastic scattering in the ring. The white dashed circle shows the expected path of the electrons passing through the ring with $D \approx 300$ nm. The ring is connected to the source and drain contacts by two 150 nm wide point contacts (marked with an ∗). The conductivity through both point contacts is mainly controlled by the voltage $V_A$ applied to IPGA. For $V_A = V_B = 0$ mV the point contacts are conducting and the resistance of the device is found to be between $h/e^2$ and $h/2e^2$. This suggests that only one conducting channel is contributing to the transport. All measurements were performed in a dilution refrigerator at a base temperature of $T = 25$ mK with a standard lock-in technique and an ac voltage of 5 $\mu$V ($f = 89$ Hz).

Figure 1(*b*) shows the conductance $G(B)$ of the quantum ring in the open regime with $V_A = 95$ mV and $V_B = 120$ mV ($R < h/e^2$) in a perpendicular magnetic field $B$. We observe AB oscillations with an amplitude of more than 50%. The power spectrum of the data in figure 1(*b*) is shown in figure 1(*c*). In the power spectrum the dominating feature is a frequency of 16 $T^{-1}$. This means that every 62 mT a flux quantum enters the area enclosed by the electron paths. From this value we can determine the diameter of the dominating electron orbit in our ring to $D = 300$ nm. This fits perfectly for the geometry as shown in figure 1(*a*) by the white dashed line. The observation of a dominant frequency at 16 $T^{-1}$ is an additional indication that only one conducting channel is present in this voltage regime.

Due to the geometry of the device it is possible to pinch-off both point contacts simultaneously with a negative voltage applied to IPGA. With $V_A = -150$ mV we create electronic barriers at the constrictions with low tunnelling transparency and are now able to study the quantum ring in the CB regime. In figure 2(*b*) two CB peaks of the structure are shown. $G(V_B)$ exhibits peaks for every electron added to the ring. By sweeping IPGB between $-200$ mV and $-170$ mV we increase the electron number $N$ on the ring to $N + 2$. The two peaks are separated by 15 mV which gives a sidegate capacitance of $C_B \approx 11$ aF. This value is consistent with values of our previous devices [12].

Figure 2(*a*) shows a greyscale plot of the source–drain current $I_{SD}$ through the ring in the CB regime. White (black) displays high (low) current. We observe nice CB diamonds as expected for a single-electron transistor. By analysing the width of the $N + 1$-diamond in figure 2(*a*) we determine the overall capacitance $C_\Sigma \approx 160$ aF corresponding to a charging energy of the ring of approximately 1 meV.

In the CB regime we also observe AB oscillations. By applying a perpendicular magnetic field we measured the change in the conductance of the second CB peak ($V_B = -177$ mV). The result is shown in figure 3(*a*) where the variation of the peak height $\Delta G(B)$ is plotted against magnetic field $B$ after subtraction of a slowly varying background. $\Delta G(B)$ shows a periodic modulation with increasing magnetic field. According to Tan and Inkson [13] one expects that the peak amplitude oscillates with each flux quantum $\Phi_0$ entering the quantum

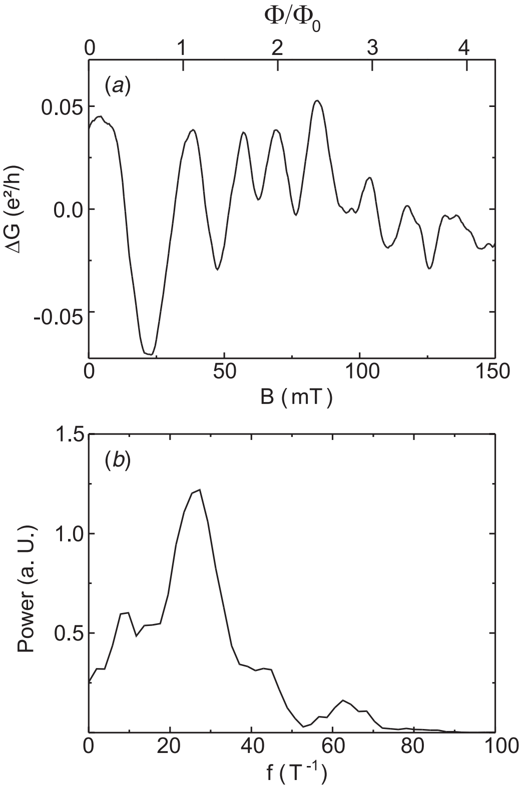


**Figure 3.** (*a*) Quasi-periodic AB oscillations of the second CB peak in figure 2(*b*) at $V_{SD} \approx 0$ mV and $V_A = -150$ mV and $V_B = -177$ mV. The change of peak height is shown after subtraction of an offset. (*b*) Power spectrum of the data in (*a*). A broad distribution is observed with a maximum at 28 $T^{-1}$.

ring. This behaviour was recently observed by Fuhrer *et al* [14] for similar fabricated quantum rings. The more complicated oscillations shown in figure 3(*a*) can be interpreted as a mixing of several electron orbits that contribute to the tunnelling transport since the ground state changes with magnetic field.

The corresponding power spectrum of $\Delta G$ presented in figure 3(*a*) is shown in figure 3(*b*). For our ring we obtain a clear peak centred at 28 $T^{-1}$ which means that every 36 mT a flux quantum enters the area surrounded by the tunnelling electrons. The corresponding electron orbit has a diameter of 380 nm which is in good agreement with the geometric dimensions of our structure. There is also a weaker mode present at 10 $T^{-1}$ for electrons cycling closer around the inner diameter of the ring ($D \approx 230$ nm). The two higher frequency components at 45 and 63 $T^{-1}$ that appear in figure 3(*b*) are due to electrons that travel twice or three times around the ring before tunnelling into the drain contact.

The design of this device with the attached IPGs allows one to measure the electrical AB [15] effect as well (data not presented here). It is also possible to tune the tunnelling barriers into an intermediate coupling regime to study the Kondo effect [16] in such quantum rings.

In conclusion, we have fabricated a sub-micrometre quantum ring structure with direct nanolithography using an AFM. In the open-transport regime we observed AB oscillations with amplitudes of more than 50%. The device was even tuned into the CB regime now showing AB-like oscillations. These rings are ideally suitable for detailed studies of phase coherent and interference effects in ballistic systems from the strong to the weak coupling regime.

## Acknowledgments

We acknowledge financial support from the BMBF. We thank F Hohls and P Hullmann for helpful discussions.

## References

[1] Aharonov Y and Bohm D 1959 *Phys. Rev.* **115** 385
[2] Ismail K, Washburn S and Lee K Y 1991 *Appl. Phys. Lett.* **59** 1998
[3] Pedersen S, Hansen A E, Kristensen A, Sorensen C B and Lindelof P E 2000 *Phys. Rev.* B **61** 5457
[4] Cassé M, Kvon Z D, Gusev G M, Olshanetsjii E B, Litvin L V, Plotnikov A V, Maude D K and Portal J C 2000 *Phys. Rev.* B **62** 2624
[5] Piazza V, Beltram F, Wegscheider W, Liang C T and Pepper M 2000 *Phys. Rev.* B **62** 10630
[6] Yacoby A, Heiblum M, Mahlu D and Shtrikman H 1995 *Phys. Rev. Lett.* **74** 4047
[7] van der Wiel W G, de Franceschi S, Fujisawa T, Elzerman J M, Tarucha S and Kouwenhoven L P 2000 *Science* **289** 2105
[8] Lorke A, Luyken R J, Govorov A O, Kotthaus J P, Garcia J M and Petroff P M 2000 *Phys. Rev. Lett.* **84** 2223
[9] Warburton R J, Schaflein C, Haft D, Bickel F, Lorke A, Karral K, Garcia J M, Schoenfeld W and Petroff P M 2000 *Nature* **405** 926
[10] Ishii M and Matsumoto K 1995 *Japan. J. Appl. Phys.* **34** 1329
[11] Held R, Vancura T, Heinzel T, Ensslin K, Holland M and Wegscheider W 1998 *Appl. Phys. Lett.* **73** 262
[12] Keyser U F, Schumacher H W, Zeitler U, Haug R J and Eberl K 2000 *Appl. Phys. Lett.* **76** 457
[13] Tan W C and Inkson J C 1996 *Semicond. Sci. Technol.* **11** 1635
[14] Fuhrer A, Lüscher S, Ihn T, Heinzel T, Ensslin K, Wegscheider W and Bichler M 2001 *Nature* **413** 822
[15] Baumgartner P, Wegscheider W, Bichler M, Groos K and Abstreiter G 1998 *Physica* E **2** 441
[16] Goldhaber-Gordon D, Shtrikman H, Mahalu D, Abusch-Magder D, Meirav U and Kastner M A 1998 *Nature* **391** 156